Memory-Event-Triggered Fault Detection of Networked IT2 T–S Fuzzy Systems

Zhou Gu, *Member, IEEE*, Dong Yue, *Fellow, IEEE*, Ju H. Park, *Senior Member, IEEE*, and Xiangpeng Xie, *Member, IEEE*

***Abstract*—In this article, a networked fault detection (FD) problem is investigated for interval type-2 T–S fuzzy systems. A novel adaptive memory-event-triggered mechanism (METM) is proposed by introducing historical information of the measured output in a prescribed sliding window. The current measured output in the traditional event-triggered mechanism is replaced by a weighting function-based historical information. As a result, the data releasing rate can be effectively reduced and maltriggering events aroused by unknown abrupt disturbance or measurement noise can be avoided as well. Meanwhile, an adaptive threshold depending on the historical information is utilized to further adjust the data releasing rate. The FD filter is designed and derived in terms of linear matrix inequalities to guarantee the H_∞ performance of fault detected systems. Finally, a hardware-in-loop simulation experiment platform is built to manifest the effectiveness of the proposed METM-based FD method.**

***Index Terms*—Fault detection (FD), interval type-2 (IT2) T–S fuzzy system, memory-event-triggered mechanism (METM).**

I. Introduction

FAULT detection (FD) plays a vital role in improving the safety and reliability of industrial process operations, such as FD in high-speed trains [1], unmanned surface vehicles [2], photovoltaic systems [3], and so on. The fault usually masked by measurement noises and disturbances is hard to be detected, which may cause unsatisfied performance or even paralysis of the system [4]–[6]. During the past few decades, FD has become an active research field, stimulating the development of various approaches and heuristics. Some meaningful results are developed on the topic of FD problems. To mention a few, in [7], an FD approach was proposed for high-voltage direct current systems by using short-time wavelet entropy. An asynchronous FD filter (FDF) was developed for 2-D Markov jump systems in [8]. Wang *et al.* [9] investigated an FD approach for parameter-varying descriptor systems by using the Yakubovich–Popov lemma to achieve a satisfactory fault evaluation performance in the finite-frequency domain. In recent years, with the development of communication technology and the expansion of control systems, network-based FD for cyber-physics systems has attracted considerable attention, see [10]–[12], and references therein.

The introduction of a communication network promotes automation and modularization due to the merits of low cost, high reliability, and ease of maintenance. For these networked control systems (NCSs), the signal is transmitted over the communication network, wherein the time-triggered mechanism (TTM) of packet releasing is wildly adopted [13]–[16]. The sampling/releasing period is usually designed to be a small enough constant to allow for the worst case of the control system. Periodical release with this small period may result in redundant packets transmitted through the network, thereby reducing the quality of service (QoS) and deteriorating the performance of control systems. Therefore, the research on saving the limited network bandwidth for NCSs, including networked FD systems, has become a hot topic.

As an alternative to TTM, the event-triggered mechanism (ETM) is an effective way to saving communication and computation resources. The ETM of NCSs has attracted considerable attention and much interesting research have been done in recent years, see [17]–[22] and the references therein. Wang and Lemmon [17] proposed an ETM, under which the subsystem information of the distributed NCS is broadcast to its neighbor's only when the state error exceeds a predetermined threshold. The ETM proposed in [18] inherits the merit of sampling control and overcomes the flaw of Zeno behavior in [17]. Under such an ETM, the set of releasing sequence belongs to that of periodic sampling sequences. Meanwhile, these meaningful results on ETM are also extended to the design of FDF. Based on [18], an FDF was designed for nonlinear systems. Although only part of the sampling packets are used to generate the residual signal in this scheme, it can obtain a satisfactory evaluation performance. Gao *et al.* [20] investigated an event-based FD problem for discrete-time networked nonlinear systems with random packet dropouts and (x, v)-dependent noises. In [21], an event-triggered FDF for the system with probability-based sensor fault was studied.

Manuscript received 6 February 2021; revised 18 December 2021; accepted 26 February 2022. Date of publication 14 March 2022; date of current version 13 January 2023. This work was supported in part by the National Natural Science Foundation of China under Grant 62022044; in part by the Jiangsu Natural Science Foundation for Distinguished Young Scholars under Grant BK20190039; and in part by the National Research Foundation of Korea (NRF) grant funded by the Korea Government (Ministry of Science and ICT) under Grant 2019R1A5A8080290. This article was recommended by Associate Editor T. H. Lee. *(Corresponding authors: Zhou Gu; Dong Yue.)*

Zhou Gu is with the College of Mechanical and Electronic Engineering, Nanjing Forestry University, Nanjing 210037, China (e-mail: gzh1808@163.com).

Dong Yue and Xiangpeng Xie are with the Institute of Advanced Technology, Nanjing University of Posts and Telecommunications, Nanjing 210023, China (e-mail: medongy@vip.163.com; xiexiangpeng1953@163.com).

Ju H. Park is with the Department of Electrical Engineering, Yeungnam University, Gyeongsan 38541, South Korea (e-mail: jessie@ynu.ac.kr).

Color versions of one or more figures in this article are available at https://doi.org/10.1109/TCYB.2022.3155755.

Digital Object Identifier 10.1109/TCYB.2022.3155755

To obtain a less conservative result, the Wirtingger inequality approach was used to achieve the parameters of FDF. In order to balance the system performance and the efficiency of data releasing, some adaptive ETMs are proposed. For example, the threshold of the ETM in [23], [24] was designed as a dynamic behavior, which is dependent on the system state. The adaptive threshold design concept is also adopted in FDF design. For example, in [25], the adaptive ETM-based FD design for nonlinear systems with sensor saturation was put forward. In [26], the FD design method for semi-Markovian Jump system with output quantization was presented using the adaptive ETM. It is noted that the literature mentioned above on the ETM uses the current information and the latest released information to determine the next releasing instant. However, using the information at a specified instant may cause unexpected triggering events. Up to now, few literature on the event triggered FD using the past period information to decide the next releasing instant, which is one of the main motivations of this study.

It is known that complex nonlinear problems widely exist in practical systems. Takagi–Sugeno (T–S) fuzzy-model-based approach is generally considered to be an effective method to characterize smooth nonlinear systems [27], [28]. By using the T–S fuzzy model, the nonlinear systems can be approximated by a convex sum of a series of local linear systems with corresponding membership functions. Therefore, the method based on the T–S fuzzy model establishes an effective link between theories of the linear and nonlinear system. Applying this approach, numerical interesting results on FD have been reported, for example, Li and Yang [29] investigated the FD problem for T–S fuzzy systems with sensor fault in the finite-frequency domain. In [30], the FD problem for T–S fuzzy systems with time-delay was addressed via delta operator approach. Dissipativity-based FD for uncertain switched T–S fuzzy systems with intermittent faults were studied in [31]. Note that the parameter uncertainty of the membership function in practical systems is commonly inevitable. Therefore, it is a big challenge for the analysis using the type-1 fuzzy models with membership functions containing no uncertainty. However, the interval type-2 (IT2) fuzzy model can well address this problem by using the information of the lower membership function (LMF) and upper membership function (UMF). Considering the uncertainty of premise variables, the IT2 fuzzy model theory was extensively employed in [32]–[37] and references therein. For example, in [36], finite-frequency FD filtering design was studied for nonlinear systems based on the IT2 fuzzy model.

Based on the above discussion, we would like to investigate the FD problem for IT2 T–S fuzzy systems under the new memory-ETM (METM) in this study. The main contribution of this article can be summarized as follows.

1) A novel METM is developed by introducing a sliding window with historical information of the measured output. Besides the latest released information, the historical information matching with a weighing function in the sliding window is utilized to be the input of the METM. Compared to the traditional ETM, the current measured output is replaced by the weighted historical information (WHI), by which it can avoid malreleasing events caused by dramatical disturbance and high-frequency measurement noise.
2) An adaptive threshold that depends on relative error with WHI is designed. Under such a scheme, the threshold decreases when the relative error increases, which implies that the probability of releasing event increases when the variation of the measured output is large enough, such that the system's performance can be maintained.
3) An integrated model of FDF for IT2 fuzzy systems considering the problem of asynchronous premise variables is established, under which the METM-based FDF design conditions are derived to implement the fault evaluation. Furthermore, a wireless network FD device based on the ZigBee protocol is developed. On such an experimental platform, the performance of the fault evaluation for IT2 fuzzy systems is verified by using our proposed method.

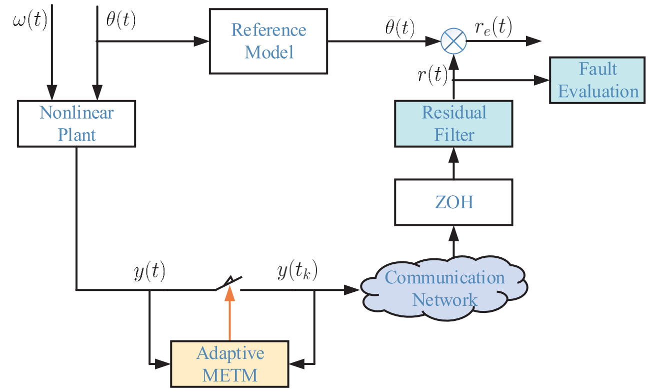

Fig. 1. Framework of networked FD systems.

Notation: In this study, $\Gamma\{M \cdot N\}$ is used to represent $N^T MN$. I_n and 0_n indicate $n \times n$ dimension identity and zero matrix, respectively. The others symbols are regular.

II. Problem Formulation

The framework of networked FD systems with adaptive METM is depicted in Fig. 1. The output signal is transmitted over the network. To alleviate the burden of communication network, an adaptive METM is adopted to determine at which instant the output is necessary for the FDF. The output will not be updated until the next event is generated by METM due to the zero-order holder (ZOH). The nonlinear plant, in this study, is characterized by an IT2 T–S fuzzy model.

The ith rule of the considered IT2 T–S fuzzy model is presented as follows.

Plant Rule i: **IF** $\varphi_1(t)$ is $G_i^1, \ldots,$ and $\varphi_q(t)$ is $G_i^{\hat{q}}$, **THEN**

$$\begin{cases} \dot{x}(t) = A_i x(t) + F_i \theta(t) + E_i \omega(t) \\ y(t) = C_i x(t) \end{cases} \tag{1}$$

for $i = 1, 2, \ldots, r$. $\varphi_j(t)$ is the jth premise variable and G_i^j denotes fuzzy set for $j = \{1, 2, \ldots, q\}$. $x(t) \in \mathbb{R}^n$ and $y(t) \in \mathbb{R}^m$ are the system state and output vectors, $\theta \in \mathbb{R}^{n_\theta}$ is a fault vector to be detected, $\omega(t) \in \mathbb{R}^{n_\omega}$ belonging to $l_2[0, \infty)$ is the disturbance, and A_i, E_i, F_i, and C_i are known matrices with appropriate dimensions. For simplification of expression, we denote $\digamma \triangleq \{1, 2, \ldots, r\}$ and $\daleth = \{1, 2, \ldots, q\}$.

Define the interval sets

$$\mathcal{M}_G^i(\varphi(t)) = \left[\underline{\mathscr{G}}_i(\varphi(t)), \overline{\mathscr{G}}_i(\varphi(t))\right] \tag{2}$$

as the firing strength of the ith rule, where $\varphi(t) = [\varphi_1(t), \ldots, \varphi_q(t)]$. LMF and UMF are, respectively, denoted by

$$\underline{\mathscr{G}}_i(\varphi(t)) = \prod_{j=1}^{q} \underline{\hbar}_{G_i^j}\big(\varphi_j(t)\big)$$
$$\overline{\mathscr{G}}_i(\varphi(t)) = \prod_{j=1}^{q} \bar{\hbar}_{G_i^j}\big(\varphi_j(t)\big).$$

Then, the final output of the IT2 T–S fuzzy model can be approximated by

$$\begin{cases} \dot{x}(t) = \sum_{i=1}^{r} \mu_i(\varphi(t))[A_i x(t) + F_i\theta(t) + E_i\omega(t)] \\ y(t) = \sum_{i=1}^{r} \mu_i(\varphi(t)) C_i x(t) \end{cases} \tag{3}$$

where the IT2 membership function $\mu_i(\varphi(t))$ is expressed by

$$\mu_i(\varphi(t)) = \frac{\partial_G^i(\varphi(t))}{\sum_{i=1}^{r}\big(\partial_G^i \varphi(t)\big)}$$

with $\partial_G^i(\varphi(t)) = \underline{m}_i(\varphi(t))\underline{\mathscr{G}}_i\varphi(t) + \overline{m}_i(\varphi(t))\overline{\mathscr{G}}_i\varphi(t)$. In the item $\partial_G^i(\varphi(t))$, $\underline{m}_i(\varphi(t))$ and $\overline{m}_i(\varphi(t))$ are nonlinear weighting functions, which satisfy $\underline{m}_i(\varphi(t)) + \overline{m}_i(\varphi(t)) = 1$, $0 < \underline{m}_i(\varphi(t)) < 1$ and $0 < \overline{m}_i(\varphi(t)) < 1$. It can be obtained that $\sum_{i=1}^{r} \mu_i(\varphi(t)) = 1$ and $0 < \mu_i(\varphi(t)) < 1$.

As shown in Fig. 1, a networked residual filter is introduced to generate fault evaluation for the nonlinear plant. The input of the residual filter $y(t_k)$ is *selected* from $y(t)$ by the adaptive METM.

Consider the jth rule of the IT2 fuzzy residual filter with the following format.

Filter Rule j: **IF** $\varsigma_1(t)$ is $H_j^1, \ldots,$ and $\varsigma_{\hat{q}}(t)$ is $H_j^{\hat{q}}$, **THEN**

$$\begin{cases} \dot{\tilde{x}}(t) = A_{fj}\tilde{x}(t) + B_{fj}y(t_k) \\ r(t) = C_{fj}\tilde{x}(t) + D_{fj}y(t_k) \end{cases} \tag{4}$$

for $t \in [t_k\ t_{k+1})$, where H_j^k and $\varsigma_j(t)$ denote fuzzy set and the jth premise variable for $j \in \digamma$, $\tilde{x}(t) \in \mathbb{R}^n$ is the state of residual filter, and $r(t)$ is the residual signal. t_k is the triggering instant. A_{fj}, B_{fj}, C_{fj}, and D_{fj} are the residual filter parameters to be designed.

Similar to the definition of the firing strength for the nonlinear plant in (2), for a residual filter, we define

$$\mathcal{N}_H^j(\varsigma(t)) = \left[\underline{\mathscr{H}}_j(\varsigma(t)), \overline{\mathscr{H}}_j(\varsigma(t))\right] \tag{5}$$

as the firing strength of the jth rule, where $\varsigma(t) = [\varsigma_1(t), \ldots, \varsigma_{\hat{q}}(t)]$, $\underline{\mathscr{H}}_j(\varsigma(t)) = \prod_{k=1}^{\hat{q}} \underline{\hbar}_{H_j^k}(\varsigma_j(t))$, and $\overline{\mathscr{H}}_j(\varsigma(t)) = \prod_{k=1}^{q} \bar{\hbar}_{H_j^k}(\varsigma_j(t))$.

Let the membership function of the residual filter be

$$\varkappa_j(\varsigma(t)) = \frac{\partial_H^j(\varsigma(t))}{\sum_{j=1}^{r}\Big(\partial_H^j \varsigma(t)\Big)} \tag{6}$$

where $\partial_H^j(\varsigma(t)) = \underline{n}_j(\varsigma(t))\underline{\mathscr{H}}_j\varsigma(t) + \overline{n}_j(\varsigma(t))\overline{\mathscr{H}}_j\varsigma(t)$. It is clear that $\sum_{i=1}^{r} \varkappa_j(\varsigma(t)) = 1$ and $0 < \varkappa_j(\varsigma(t)) < 1$.

In (6), $\underline{n}_j(\varsigma(t))$ and $\overline{n}_j(\varsigma(t))$ are nonlinear weighting functions that satisfy $\underline{n}_j(\varsigma(t)) + \overline{n}_j(\varsigma(t)) = 1$, $0 < \underline{n}_j(\varsigma(t)) < 1$, and $0 < \overline{n}_j(\varsigma(t)) < 1$.

Then, the final dynamic of the IT2 T–S fuzzy residual filter can be expressed by

$$\begin{cases} \dot{\tilde{x}}(t) = \sum_{j=1}^{r} \varkappa_j(\varphi(t_k))\big[A_{fj}\tilde{x}(t) + B_{fj}y(t_k)\big], \\ r(t) = \sum_{j=1}^{r} \varkappa_j(\varphi(t_k))\big[C_{fj}\tilde{x}(t) + D_{fj}y(t_k)\big]. \end{cases} \tag{7}$$

The input of residual filter is transmitted over the network, which is depicted in Fig. 1. To reduce the amount of data transmission while maintaining the performance of fault evaluation, the adaptive METM is introduced in the framework of networked FD.

First, we design a new vector to represent WHI of the measurement output as follows:

$$\tilde{y}_0(t) = \int_{t-\varrho}^{t} p_0(s-t)y(s)ds \tag{8}$$

where $p_0(s)$ represents an output weight that satisfies $\int_{-\varrho}^{0} p_0(s)ds = 1$.

Then, the new continuous-type memory ETM can be designed as follows:

$$t_{k+1} = \inf_{t>t_k}\{t|\phi(\varepsilon(t), y(t_k)) > 0\} \tag{9}$$

with $\phi(\varepsilon(t), y(t_k)) = \varepsilon^T(t)M\varepsilon(t) - \varpi(t)y^T(t_k)My(t_k) + \delta$, where $\varepsilon(t) = \tilde{y}_0(t) - y(t_k)$, δ is a small positive constant, and $\varpi(t)$ is defined by

$$\varpi(t) = \underline{\varpi} + \big(\varpi - \underline{\varpi}\big)e^{-\beta\|\hat{\varepsilon}(t)\|^2} \tag{10}$$

for $t \in [t_k,\ t_{k+1})$ with $0 < \underline{\varpi} < \varpi < 1, \beta > 0$, and $\hat{\varepsilon}(t) = ([\varepsilon^T(t)M\varepsilon(t)]/[y^T(t_k)My(t_k)])$.

Remark 1: From (8) and (9), one can see the state error $\varepsilon(t)$ is not an error between the current measurement and the latest releasing measurement as that in the traditional ETM. In this study, the expectation of the measurement in the sliding window from the $t-\varrho$ to t is obtained with the assumption of $\int_{-\varrho}^{0} p_0(s)ds = 1$. The WHI during the past period is introduced to replace the current measurement in the traditional ETM. Therefore, we call this mechanism METM.

Remark 2: By using the proposed METM with historical information, malreleasing event caused by dramatical disturbance or high-frequency measurement noise can be reduced due to the introduction of sliding window technique.

Remark 3: The threshold of the proposed METM $\varpi(t)$ in (10) depends on the relative error $\hat{\varepsilon}(t)$ for $t \in [t_k\ t_{k+1})$, that is, the probability of a generation of releasing event will increase when the expectation of the measurement in the sliding window deviates the value at the latest releasing instant t_k.

Remark 4: The width of the sliding window ϱ is a given constant. When ϱ is chosen too big, the releasing event will not be sensitive to the measurement variation, while it is chosen too small, such as $\varrho \to 0$, then it will be reduced to the traditional ETM due to the property that $\lim_{\varrho\to 0}(1/\varrho)\tilde{y}_0(t) = y(t)$.

For convenience of using the WHI, we define a new vector

$$\mathscr{X}(t) \triangleq \int_{t-\varrho}^{t} \mathscr{P}(s-t)x(s)ds = \int_{-\varrho}^{0} \mathscr{P}(s)x(t+s)ds \tag{11}$$

where $\mathscr{P}(s) = p(s) \otimes I_n$ and $p(s) = \mathbf{col}\{p_0(s), p_1(s), \ldots, p_{a-1}(s)\}$. Moreover, $\mathscr{P}(s)$ has the following property that will be used for the derivative of $\mathscr{X}(t)$:

$$\dot{\mathscr{P}}(s) = \mathbb{P}\mathscr{P}(s) \tag{12}$$

where $\mathbb{P}$ is a constant matrix.

Combining (8) and (11) yields that

$$\begin{aligned}\tilde{y}_0(t) &= \sum_{i=1}^{r} \mu_i(\varphi(t))C_i \int_{t-\varrho}^{t} p_0(s-t)x(s)ds \\ &= \sum_{i=1}^{r} \mu_i(\varphi(t))C_i\mathbb{H}_0\mathscr{X}(t)\end{aligned} \tag{13}$$

where $\mathbb{H}_0 = [I_n \; 0_{n\times(a-1)n}]$.

From the definition of $\varepsilon(t)$, it has

$$y(t_k) = \sum_{i=1}^{r} \mu_i(\varphi(t))C_i\mathbb{H}_0\mathscr{X}(t) - \varepsilon(t). \tag{14}$$

Inspired by [38], a reference model for the fault signal is introduced (see Fig. 1) to generate an expected residual evaluation result. The transfer function from fault signal $\theta(t)$ to $\bar{\theta}(t)$ is designed by $G_\theta(s) = [\bar{\theta}(s)/\theta(s)]$, whose state space can be expressed by

$$\begin{cases}\dot{x}_\theta(t) = A_\theta x(t) + B_\theta\theta(t) \\ \bar{\theta}(t) = C_\theta x_\theta(t) + D_\theta\theta(t).\end{cases} \tag{15}$$

Define $\eta(t) = [x^T(t) \; \tilde{x}^T(t) \; x_\theta^T(t)]^T$, $\vartheta(t) = [\omega^T(t) \; \theta^T(t)]^T$, and $r_e(t) = r(t) - \bar{\theta}(t)$. Then, based on (3), (7), and (14), one can obtain the following overall system:

$$\begin{cases}\dot{\eta}(t) &= \sum_{i=1}^{r}\mu_i(\varphi(t))\varkappa_j(\varphi(t_k))\big[\mathcal{F}_{1ij}\eta(t) + \mathcal{F}_{2ij}\mathscr{X}(t) \\ &\quad +\mathcal{F}_{3j}\varepsilon(t) + \mathcal{F}_{4i}\vartheta(t)\big], \\ r_e(t) &= \sum_{i=1}^{r}\mu_i(\varphi(t))\varkappa_j(\varphi(t_k))\big[\mathcal{G}_{1j}\eta(t) + \mathcal{G}_{2ij}\mathscr{X}(t) \\ &\quad +\mathcal{G}_{3j}\varepsilon(t) + \mathcal{G}_4\vartheta(t)\big]\end{cases} \tag{16}$$

where

$$\mathcal{F}_{1ij} = \begin{bmatrix} A_i & 0 & 0 \\ 0 & A_{fj} & 0 \\ 0 & 0 & A_\theta \end{bmatrix}, \; \mathcal{F}_{2ij} = \begin{bmatrix} 0 \\ B_{fj}C_i\mathbb{H}_0 \\ 0 \end{bmatrix},$$

$$\mathcal{F}_{3j} = \begin{bmatrix} 0 \\ B_{fj} \\ 0 \end{bmatrix}, \mathcal{F}_{4i} = \begin{bmatrix} E_i & F_i \\ 0 & 0 \\ 0 & B_\theta \end{bmatrix}, \; \mathcal{G}_{1j} = \begin{bmatrix} 0 & C_{fj} & -C_\theta \end{bmatrix},$$

$$\mathcal{G}_{2ij} = D_{fj}C_i\mathbb{H}_0, \; \mathcal{G}_{3j} = -D_{fj}, \; \mathcal{G}_4 = [0 \quad -D_\theta].$$

For expression brief, in what follows, we will use μ_i^t and $\varkappa_j^k$ to represent $\mu_i(\varphi(t))$ and $\varkappa_j(\varphi(t_k))$ in (16), respectively. Moreover, the condition $\mu_i^t - \alpha_j\varkappa_j^k \geq 0$ is assumed to be hold.

Next, we introduce a residual evaluation function (REF) $J(t)$ as follows:

$$J(t) = \left(\int_0^t \|r(s)\|^2 ds\right)^{\frac{1}{2}}. \tag{17}$$

To detect the fault occurrence, an FD threshold J_{th} needs to be preset, which is expressed by

$$J_{th} = \sup_{\omega(t)\in L_2, \theta(t)=0} J(t). \tag{18}$$

Based on the REF in (17) and the FD threshold in (18), the following FD logic is adopted:

$$\begin{cases} J(t) > J_{th} \Rightarrow \text{alarm} \\ J(t) \leq J_{th}. \end{cases} \tag{19}$$

The main objective of this article is to find FD parameters in (7) such that:

1) the FD system (16) is uniformly ultimately bounded (UUB);
2) under the zero-initial condition, $\int_0^t r_e^T(s)r_e(s)ds \leq \gamma^2\int_0^t \vartheta^T(s)\vartheta(s)ds$ with $\vartheta(t) \in l_2[0, +\infty)$ is satisfied for the solution of (16), where γ is a positive scalar.

III. Fault Detection Filter Design

In this section, an H_∞ performance analysis for the FDF system under the adaptive METM will be presented first. Then, we will design the parameters of the IT2 fuzzy FDF in (7) in the light of Theorem 2.

To facilitate deriving the result in Theorem 1, the following Lemma is introduced.

Lemma 1 [22]: For a vector $p(s)$ defined in (11), symmetric matrix $R > 0$, one has

$$\int_{\mathcal{D}} \Gamma\{R \cdot x(s)\}ds \geq \Gamma\{\mathcal{R} \cdot \mathscr{X}(t)\} \tag{20}$$

where $\mathcal{R} = P \otimes R$ with $P = [\int_{-\varrho}^{0} p(s)p^T(s)ds]^{-1}$, and $\mathscr{X}(x)$ is defined in (11).

Theorem 1: For given positive constants $\alpha_j, \beta, \varrho, \varpi$, and γ and matrices C_{fj}, D_{fj}, and T, the IT2 fuzzy-based residual system (16) under the adaptive METM in (9) is asymptotically stable with an H_∞ norm bound γ, if there exist symmetric matrices $Q, \Phi_{ij} > 0, R > 0, S > 0$, and $M > 0$, and matrices A_{fj} and B_{fj}, such that the following inequalities hold:

$$\Pi_{ij} - \Phi_{ij} < 0 \tag{21}$$

$$\Upsilon_{ii} < 0 \tag{22}$$

$$\Upsilon_{ij} + \Upsilon_{ji} \leq 0, \qquad i < j \tag{23}$$

$$\mathcal{Q} > 0 \tag{24}$$

for $i, j \in \digamma$, where

$$\begin{aligned}\Upsilon_{ij} &= \Phi_{ij} + \alpha_j\big(\Pi_{ij} - \Phi_{ij}\big) \\ \Pi_{ij} &= \Gamma\{(R + \varrho S) \cdot \mathbb{H}_1\mathbb{J}_1\} - \Gamma\{R \cdot \mathbb{J}_2\} - \Gamma\{\mathcal{S} \cdot \mathbb{H}_2\mathbb{J}_1\} \\ &\quad + \Gamma\Big\{\delta^3 I \cdot \mathbb{H}_3\mathbb{J}_1\Big\} + \mathbf{He}\Big\{\mathbb{J}_1^T Q\begin{bmatrix}\mathfrak{I} \\ \mathfrak{P}\end{bmatrix}\Big\} - \Gamma\{M \cdot \mathbb{J}_3\} \\ &\quad + \Gamma\{\varpi M \cdot [C_i\mathbb{H}_0\mathbb{H}_2\mathbb{J}_1 - \mathbb{J}_3]\} \\ &\quad + \mathbf{He}\{\mathcal{T}\mathfrak{F}_{ij}\} + \mathfrak{G}_{ij}^T\mathfrak{G}_{ij} - \gamma^2\mathbb{J}_4^T\mathbb{J}_4\end{aligned}$$

$$\begin{aligned}
\mathcal{T} &= \begin{bmatrix} T & 0_{n_\eta \times (an+n+m+n_\vartheta)} & \beta T \end{bmatrix}\\
\mathcal{Q} &= Q + diag\{0, \mathcal{R}\}, \quad \mathcal{S} = P \otimes S\\
\mathcal{R} &= P \otimes R, \quad P = \left[\int_{-\varrho}^{0} p(s)p^T(s)ds\right]^{-1}\\
\mathcal{F}_{ij} &= \begin{bmatrix} \mathcal{F}_{1ij} & \mathcal{F}_{2ij} \end{bmatrix}, \; \mathcal{G}_{ij} = \begin{bmatrix} \mathcal{G}_{1j} & \mathcal{G}_{2ij} \end{bmatrix}\\
\mathbb{H}_1 &= \begin{bmatrix} I_n & 0_n & 0_{n\times n_\theta} & 0_{n\times an} \end{bmatrix}, \mathbb{H}_2 = \begin{bmatrix} 0_{an\times n} & 0_{an\times n} & 0_{an\times n_\theta} & I_{an} \end{bmatrix}\\
\mathbb{H}_3 &= \begin{bmatrix} I_{n_\eta} & 0_{n_\eta\times an} \end{bmatrix}, \; \mathcal{Y} = \begin{bmatrix} \mathscr{P}(0) & 0_{an\times n} & 0_{an\times n_\theta} & -\mathbb{P} \end{bmatrix}\\
\mathfrak{P} &= \begin{bmatrix} \mathcal{Y} & -\mathscr{P}(-\varrho) & 0_{an\times m} & 0_{an\times n_\vartheta} & 0_{an\times n_\eta} \end{bmatrix}\\
\mathfrak{I} &= \begin{bmatrix} 0_{n_\eta\times n_\zeta} & 0_{n_\eta\times n} & 0_{n_\eta\times m} & 0_{n_\eta\times n_\vartheta} & I_{n_\eta} \end{bmatrix}\\
\mathfrak{F}_{ij} &= \begin{bmatrix} \mathcal{F}_{ij} & 0 & \mathcal{F}_{3j} & \mathcal{F}_{4i} & -I \end{bmatrix}, \; \mathfrak{G}_{ij} = \begin{bmatrix} \mathcal{G}_{ij} & 0 & \mathcal{G}_{3j} & \mathcal{G}_4 & 0 \end{bmatrix}\\
\mathbb{J}_1 &= \begin{bmatrix} I_{n_\zeta} & 0_{n_\zeta\times n} & 0_{n_\zeta\times m} & 0_{n_\zeta\times n_\vartheta} & 0_{n_\zeta\times n_\eta} \end{bmatrix}\\
\mathbb{J}_2 &= \begin{bmatrix} 0_{n\times n_\zeta} & I_{n\times n} & 0_{n\times m} & 0_{n\times n_\vartheta} & 0_{n\times n_\eta} \end{bmatrix}\\
\mathbb{J}_3 &= \begin{bmatrix} 0_{m\times n_\zeta} & 0_{m\times n} & I_{m\times m} & 0_{m\times n_\vartheta} & 0_{m\times n_\eta} \end{bmatrix}\\
\mathbb{J}_4 &= \begin{bmatrix} 0_{n_\vartheta\times n_\zeta} & 0_{n_\vartheta\times n} & 0_{n_\vartheta\times m} & I_{n_\vartheta\times n_\vartheta} & 0_{n_\vartheta\times n_\eta} \end{bmatrix}\\
\mathbb{J}_5 &= \begin{bmatrix} 0_{n_\eta\times n_\zeta} & 0_{n_\eta\times n} & 0_{n_\eta\times m} & 0_{n_\eta\times n_\vartheta} & I_{n_\eta\times n_\eta} \end{bmatrix}\\
n_\zeta &= n_\eta + an, n_\vartheta = n\omega + n_f, n_\eta = 2n + n_\theta.
\end{aligned}$$

Proof: Construct the LKF as follows:

$$V(t) = V_1(t) + V_2(t) + V_3(t) \tag{25}$$

where

$$\begin{aligned}
V_1(t) &= \varGamma\{Q \cdot \zeta(t)\}\\
V_2(t) &= \int_{t-\varrho}^{t} \varGamma\{R \cdot \mathbb{H}_1\zeta(s)\}ds\\
V_3(t) &= \int_{t-\varrho}^{t} (s - t + \varrho)\varGamma\{S \cdot \mathbb{H}_1\zeta(s)\}ds
\end{aligned}$$

with $\zeta(t) = [\eta^T(t) \;\; \mathscr{X}^T(t)]^T$.

From Lemma 1, one can know that

$$V_2(t) \ge \varGamma\{\mathcal{R} \cdot \mathscr{X}(t)\}. \tag{26}$$

Due to $\mathcal{Q} > 0$ and $S > 0$, we have

$$V(t) \ge \varGamma\{\mathcal{Q} \cdot \zeta(t)\} + \int_{-\varrho}^{0} (s + \varrho)\varGamma\{S \cdot x(t + s)\}ds > 0. \tag{27}$$

From (27), one knows that if (24) is satisfied, $Q > 0$ is not yet required. Therefore, a less conservative result can be obtained.

Taking the derivative of $V(t)$ along the residual system (16) yields that

$$\begin{aligned}
\dot{V}(t) = {}& 2\zeta^T(t)Q\dot{\zeta}(t) + \varGamma\{R \cdot x(t)\} - \varGamma\{R \cdot x(t - \varrho)\}\\
&+ \varrho\varGamma\{S \cdot x(t)\} - \int_{t-\varrho}^{t} \varGamma\{S \cdot x(s)\}ds.
\end{aligned}$$

From (11) and (12), it follows that:

$$\begin{aligned}
\dot{\mathscr{X}}(t) &= \mathscr{P}(0)x(t) - \mathscr{P}(-\varrho)x(t - \varrho) - \mathbb{P}\mathscr{X}(t)\\
&\triangleq \mathscr{Y}(t).
\end{aligned} \tag{28}$$

Similar to (26), applying Lemma 1 follows that:

$$-\int_{t-\varrho}^{t} \varGamma\{S \cdot x(s)\}ds \le -\varGamma\{\mathcal{S} \cdot \mathscr{X}(x)\}. \tag{29}$$

Recalling the definition of $\varepsilon(t)$ in (9) and (14), it has $\phi(\varepsilon(t), y(t_k)) < 0$ is equivalent to

$$\begin{aligned}
&\sum_{i=1}^{r} \mu_i^t\Big[\varpi\varGamma\big\{M \cdot \big[C_i\mathbb{H}_0\mathscr{X}(x) - \varepsilon(t)\big]\big\}\\
&\qquad -\varGamma\{M \cdot \varepsilon(t)\} + \delta\Big] > 0.
\end{aligned} \tag{30}$$

For notational simplification, we define $\psi(t) = [\zeta^T(t) \; x^T(t-\varrho) \; \varepsilon^T(t) \; \vartheta^T(t) \; \dot{\eta}^T(t)]^T$.

Then, it has

$$\begin{aligned}
\dot{V}(t) < {}& \sum_{i=1}^{r} \mu_i^t\varkappa_j^k\big[\varGamma\{R \cdot x(t)\} - \varGamma\{R \cdot x(t - \varrho)\}\big]\\
&+ \sum_{i=1}^{r} \mu_i^t\varkappa_j^k\big[\varGamma\{\varrho S \cdot x(t)\} - \varGamma\{\mathcal{S} \cdot \mathscr{X}(t)\}\big]\\
&+ \sum_{i=1}^{r} \mu_i^t\varkappa_j^k\left[2\zeta^T(t)Q\begin{bmatrix} \dot{\eta}(t)\\ \mathscr{Y}(t) \end{bmatrix} - \varGamma\{M \cdot \varepsilon(t)\}\right]\\
&+ \sum_{i=1}^{r} \mu_i^t\varkappa_j^k\big[\varGamma\big\{\varpi M \cdot \big[C_i\mathbb{H}_0\mathscr{X}(x) - \varepsilon(t) + \delta\big]\big\}\big]\\
&+ \sum_{i=1}^{r} \mu_i^t\varkappa_j^k \; 2\varGamma\big\{\mathcal{T}\mathfrak{F}_{ij} \cdot \psi(t)\big\}.
\end{aligned}$$

Then, we can obtain that

$$\begin{aligned}
&\dot{V}(t) + r_e^T(t)r_e(t) - \gamma^2\vartheta^T(t)\vartheta(t) + \delta^3\eta^T(t)\eta(t)\\
&\quad + \delta - \delta^3\eta^T(t)\eta(t) \le \sum_{i=1}^{r} \mu_i^t\varkappa_j^k\varGamma\big\{\Pi_{ij} \cdot \psi(t)\big\}.
\end{aligned} \tag{31}$$

It is noted that $\sum_{i=1}^{r}\sum_{j=1}^{r} \mu_i^t(\mu_i^t - \varkappa_j^k) = 0$. Then, for matrix Φ_{ij} with an appropriate dimension, we have

$$\begin{aligned}
\sum_{i=1}^{r} \mu_i^t\varkappa_j^k\varGamma\big\{\Pi_{ij} \cdot \psi(t)\big\} = {}& \sum_{i=1}^{r} \mu_i^t\varkappa_j^k\varGamma\big\{\Pi_{ij} \cdot \psi(t)\big\}\\
&+ \sum_{i=1}^{r}\sum_{j=1}^{r} \mu_i^t\Big(\mu_i^t - \varkappa_j^k\Big)\varGamma\big\{\Phi_{ij} \cdot \psi(t)\big\}\\
= {}& \sum_{i=1}^{r}\sum_{j=1}^{r} \mu_i^t\varkappa_j^k\varGamma\big\{\big(\Pi_{ij} - \Phi_{ij}\big) \cdot \psi(t)\big\}\\
&+ \sum_{i=1}^{r}\sum_{j=1}^{r} \mu_i^t\varkappa_j^t\varGamma\big\{\Phi_{ij} \cdot \psi(t)\big\}.
\end{aligned} \tag{32}$$

Recalling the assumption of $\mu_j^k - \alpha_j\varkappa_j^t \ge 0$, (21), and the definition of Υ_{ij} in Theorem 1, it has

$$\sum_{i=1}^{r}\sum_{j=1}^{r} \mu_i^t\varkappa_j^k\varGamma\big\{\Pi_{ij} \cdot \psi(t)\big\} \le \sum_{i=1}^{r}\sum_{j=1}^{r} \mu_i^t\varkappa_j^t\varGamma\big\{\Upsilon_{ij} \cdot \psi(t)\big\}. \tag{33}$$

Using parameterized linear matrix inequality technique [39] follows that:

$$\begin{aligned}
\sum_{i=1}^{r}\sum_{j=1}^{r} \mu_i^t\varkappa_j^k\varGamma\big\{\Pi_{ij} \cdot \psi(t)\big\} \le {}& \sum_{i=1}^{r} \mu_i^t\mu_i^t\varGamma\{\Upsilon_{ii} \cdot \psi(t)\}\\
&+ \sum_{i=1}^{r}\sum_{j>i}^{r} \mu_i^t\mu_i^t\varGamma\big\{\big(\Upsilon_{ij} + \Upsilon_{ji}\big) \cdot \psi(t)\big\}.
\end{aligned} \tag{34}$$

Combining (22), (23), (31), and (34) yields that when $\|\eta(t)\| > \delta^2$,

$$\dot{V}(t) \leq -r_e^T(t)r_e(t) + \gamma^2\vartheta^T(t)\vartheta(t). \tag{35}$$

For $\vartheta(t) = 0$, it is easily known that $\dot{V}(t) < 0$ from (35), which means the residual system (16) is UUB.

For $\vartheta(t) \neq 0$, it follows that $\int_0^t r_e^T(s)r_e(s)ds \leq \gamma^2\int_0^t \vartheta^T(s)\vartheta(s)ds$ by integrating both sides of (35) from $0 \to t$. That completes the proof. ■

Next, we are in position to design the parameters of the FDF system in (7).

Theorem 2: For given positive constants $\alpha_j, \beta, \varrho, \varpi$, and γ, and matrices W, the IT2 fuzzy-based residual system (16) under the adaptive METM (9) is asymptotically stable with an H_∞ norm bound γ, if there exist symmetric matrices $T_2, Q, \Phi_{ij} > 0, R > 0, S > 0$, and $M > 0$ and matrices $\hat{A}_{fj}, \hat{B}_{fj}, C_{fj}, D_{fj}$, and T_k $(k = 1, 3, 4, 6, 7, 9)$, such that the following linear matrix inequalities hold:

$$\begin{bmatrix} \hat{\Pi}_{ij} - \Phi_{ij} & * \\ \mathfrak{G}_{ij} & -I \end{bmatrix} < 0 \tag{36}$$

$$\begin{bmatrix} \hat{\Upsilon}_{ii} & * \\ \mathfrak{G}_{ii} & -\sqrt{1+\alpha_i I} \end{bmatrix} < 0 \tag{37}$$

$$\begin{bmatrix} \hat{\Upsilon}_{ij} + \hat{\Upsilon}_{ji} & * & * \\ \mathfrak{G}_{ij} & -\sqrt{1+\alpha_j I} & * \\ \mathfrak{G}_{ji} & 0 & -\sqrt{1+\alpha_i I} \end{bmatrix} \leq 0,\ i < j, \tag{38}$$

$$\mathcal{Q} > 0 \tag{39}$$

for $i, j \in \digamma$, where $\mathcal{Q}, \mathcal{S}, \mathcal{G}_{ij}, P, \mathcal{R}, \mathfrak{P}$, and $\mathfrak{G}_{ij}$ are defined in Theorem 1, and

$$\begin{aligned}
\hat{\Upsilon}_{ij} &= \hat{\Pi}_{ij} + \alpha_j\left(\hat{\Pi}_{ij} - \Phi_{ij}\right)\\
\hat{\Pi}_{ij} &= \Gamma\{(R + \varrho S)\cdot \mathbb{H}_1\mathbb{J}_1\} - \Gamma\{R\cdot \mathbb{J}_2\} - \Gamma\{\mathcal{S}\cdot \mathbb{H}_2\mathbb{J}_1\}\\
&\quad + \Gamma\left\{\delta^3 I\cdot \mathbb{H}_3\mathbb{J}_1\right\} + \mathbf{He}\left\{\mathbb{J}_1^T Q\begin{bmatrix}\mathfrak{I}\\ \mathfrak{P}\end{bmatrix}\right\} - \Gamma\{M\cdot \mathbb{J}_3\}\\
&\quad + \Gamma\{\varpi M\cdot [C_i\mathbb{H}_0\mathbb{H}_2\mathbb{J}_1 - \mathbb{J}_3]\}\\
&\quad + \mathbf{He}\left\{\hat{\mathcal{T}}\hat{\mathfrak{F}}_{ij}\right\} - \gamma^2\mathbb{J}_4^T\mathbb{J}_4\\
\hat{\mathcal{T}} &= \begin{bmatrix} I & 0_{2n\times(an+n+m+n_\vartheta)} & \beta I\end{bmatrix}\\
\hat{\mathfrak{F}}_{ij} &= \left[\hat{\mathcal{F}}_{ij}\ 0\ \hat{\mathcal{F}}_{3j}\ \hat{\mathcal{F}}_{4i}\ -T\right],\ \hat{\mathcal{F}}_{ij} = \left[\hat{\mathcal{F}}_{1ij}\ \ \hat{\mathcal{F}}_{2ij}\right]\\
\hat{\mathcal{F}}_{1ij} &= \begin{bmatrix} T_1A_i & \hat{A}_{fj} & T_3A_\theta\\ T_4A_i & \hat{A}_{fj} & T_6A_\theta\\ T_7A_i & W\hat{A}_{fj} & T_9A_\theta\end{bmatrix},\ \hat{\mathcal{F}}_{2ij} = \begin{bmatrix}\hat{B}_{fj}C_i\mathbb{H}_0\\ \hat{B}_{fj}C_i\mathbb{H}_0\\ W\hat{B}_{fj}C_i\mathbb{H}_0\end{bmatrix}\\
\hat{\mathcal{F}}_{3j} &= \begin{bmatrix}\hat{B}_{fj}\\ \hat{B}_{fj}\\ W\hat{B}_{fj}\end{bmatrix},\ \hat{\mathcal{F}}_{4i} = \begin{bmatrix} T_1E_i & T_1F_i + T_3B_\theta\\ T_4E_i & T_4F_i + T_6B_\theta\\ T_7E_i & T_7F_i + T_9B_\theta\end{bmatrix}.
\end{aligned}$$

Moreover, the FDF parameters in (7) are given by

$$\left[\begin{array}{c|c} A_{fj} & B_{fj}\\ \hline C_{fj} & D_{fj}\end{array}\right] = \left[\begin{array}{c|c} T_2^{-1}\hat{A}_{fj} & T_2^{-1}\hat{B}_{fj}\\ \hline C_{fj} & D_{fj}\end{array}\right]. \tag{40}$$

Proof: Define $T = \begin{bmatrix} T_1 & T_2 & T_3\\ T_4 & T_2 & T_6\\ T_7 & WT_2 & T_9\end{bmatrix}$, $\hat{A}_{fj} = T_2A_{fj}$, and $\hat{B}_{fj} = T_2B_{fj}$.

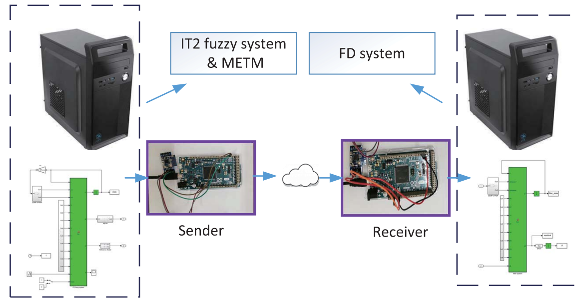

Fig. 2. Simulation platform of the FD system.

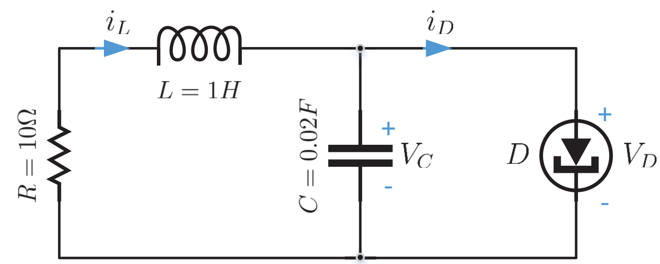

Fig. 3. Tunnel diode circuit.

From the definition of $\hat{\mathcal{T}}$ and $\hat{\mathfrak{F}}_{ij}$ in Theorem 2, one can know that (21) is equivalent to

$$\hat{\Pi}_{ij} - \Phi_{ij} + \mathfrak{G}_{ij}^T\mathfrak{G}_{ij} < 0. \tag{41}$$

Applying Schur complement yields that (41) is equivalent to (36). Equations (37) and (38) can be got by using a similar method. The proof is completed. ■

IV. Simulation Experiment

In this section, a hardware-in-loop simulation experiment is given to demonstrate the effectiveness of the proposed approach. As depicted in Fig. 2, the simulation platform is composed by three parts: 1) nonlinear plant; 2) adaptive METM, FD; and 3) wireless sending/receiving device, where the first two parts are realized by computer simulation and the signal transmission in the third part is implemented by circuits that are mainly composed of Arduino and ZigBee modules. That is, the modules of the plant and the FDF are simulated on the Simulation/MATLAB platform, while communication between these two modules is transmitted via a wireless network.

Example 1: A tunnel diode circuit is considered in this example, which is presented in Fig. 3.

The V-I characteristics of tunnel diode D is given by

$$i_D(t) = 0.002V_D(t) + \sigma V_D^3(t)$$

where $\sigma \in [0.01, 0.03]$ is an uncertain parameter and the voltage of tunnel diode satisfies $V_D(t) \in [-3\text{ V}, 3\text{ V}]$.

The application of Kirchhoff's law to Fig. 3 yields

$$\begin{cases} C\frac{dV_D}{dt} + i_D - i_L = 0\\ Ri_L + L\frac{di_L}{dt} + V_D = 0.\end{cases} \tag{42}$$

TABLE I
UMF AND THE LMF OF THE PLANT

	$\mathscr{G}_1^1(x_1(t))$	$\mathscr{G}_2^1(x_1(t))$
UMF	$\bar{\mathscr{G}}_1^1(x_1(t)) = \frac{d_{\max}-d(t)}{d_{\max}-d_{\min}}$ (with $\sigma = 0.01$)	$\bar{\mathscr{G}}_2^1(x_1(t)) = \frac{d(t)-d_{\min}}{d_{\max}-d_{\min}}$ (with $\sigma = 0.03$)
LMF	$\underline{\mathscr{G}}_1^1(x_1(t)) = \frac{d_{\max}-d(t)}{d_{\max}-d_{\min}}$ (with $\sigma = 0.03$)	$\underline{\mathscr{G}}_2^1(x_1(t)) = \frac{d(t)-d_{\min}}{d_{\max}-d_{\min}}$ (with $\sigma = 0.01$)

TABLE II
UMF AND THE LMF OF THE FDF

	$\mathscr{H}_1^1(x_1(t))$	$\mathscr{H}_2^1(x_1(t))$
UMF	$\bar{\mathscr{H}}_1^1(x_1(t))=e^{-0.2x_1^2(t)}$	$\bar{\mathscr{H}}_2^1(x_1(t))=1-e^{-0.5x_1^2(t)}$
LMF	$\underline{\mathscr{H}}_1^1(x_1(t))=e^{-0.5x_1^2(t)}$	$\underline{\mathscr{H}}_2^1(x_1(t))=1-e^{-0.2x_1^2(t)}$

Suppose there are common/differential mode noise and fault signal in the circuit. Let $x_1(t) = V_D(t), x_2(t) = i_L(t)$ and $x(t) = \begin{bmatrix} x_1(t) \\ x_2(t) \end{bmatrix}$. Then, the nonlinear dynamic of the tunnel diode circuit can be expressed by

$$\dot{x}(t) = A(t)x(t) + F\theta(t) + E\omega(t) \quad (43)$$

where

$$A(t) = \begin{bmatrix} -50d(t) & 50 \\ -1 & -10 \end{bmatrix}$$

with $d(t) = 0.002 + \sigma V_D^2$.

By using the IT2 fuzzy modeling method [40], we can convert the nonlinear tunnel diode circuit system (43) into the IT2 fuzzy system in the form of (3), and the system matrices are defined by

$$A_i = \begin{bmatrix} -50d_i & 50 \\ -1 & -10 \end{bmatrix}$$

where $d_1 = d_{\min} = 0.002$ and $d_2 = d_{\max} = 0.272$. The other matrices are chosen as

$$C_i = \begin{bmatrix} 1 \\ 0 \end{bmatrix}, E_i = \begin{bmatrix} 0 \\ 1 \end{bmatrix}, F_i = \begin{bmatrix} 1 \\ 1 \end{bmatrix}, \quad (i = 1, 2).$$

The transfer function of weighted fault dynamic in (15) is: $G_\theta(s) = -[(0.02s + 0.54)/(s + 2)]$. The UMF and the LMF of the plant and the FDF are displayed in Tables I and II, respectively.

In addition, the nonlinear weighting functions of the plant and FDF are given by $\underline{m}_i(x_1(t)) = \sin^2(x_1(t)), \overline{m}_i(x_1(t)) = 1 - \sin^2(x_1(t))$, $\underline{n}_i(x_1(t)) = \underline{m}_i(x_1(t))$, and $\overline{n}_i(x_1(t)) = \overline{m}_i(x_1(t))$, respectively.

Remark 5: As shown in Fig. 2, the IT2 fuzzy system, FDF and METM are simulated by using MATLAB. The signal transmission device is a real wireless network. Such a hardware-in-loop simulation platform can not only simplify the complexity of the experiment but also observe the real performance of networked FD.

From Theorem 2 with parameters $\delta = 0.001, \alpha_1 = 0.3, \alpha_2 = 0.7, \gamma = 2, \varrho = 0.15, \underline{\varpi} = 0.01, \bar{\varpi} = 0.2$, and $W = [1\ 1]$, one can obtain

$$A_{f1} = \begin{bmatrix} -1.7610 & 14.7975 \\ -0.2676 & -4.1922 \end{bmatrix}, B_{f1} = \begin{bmatrix} -1.5747 \\ 0.0972 \end{bmatrix}$$

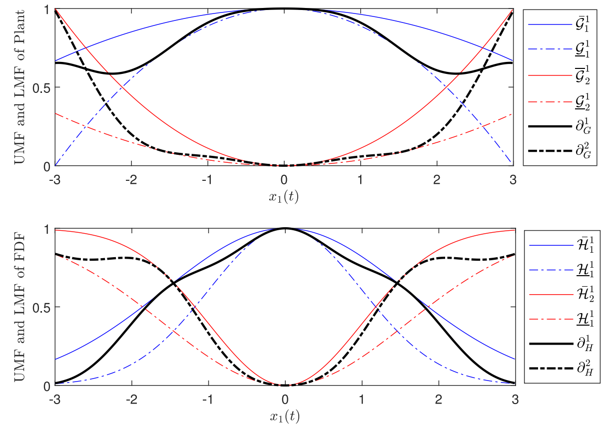

Fig. 4. Membership function of the plant and the FDF.

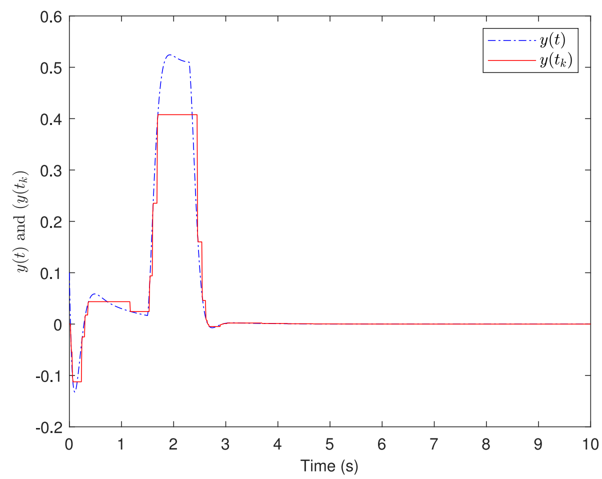

Fig. 5. Output of the plant and the input of the FDF.

$$A_{f2} = \begin{bmatrix} -20.7679 & 28.7842 \\ 0.9881 & -5.8199 \end{bmatrix}, B_{f2} = \begin{bmatrix} 0.4940 \\ 0.2717 \end{bmatrix}$$

$$C_{f1} = \begin{bmatrix} -0.0247 & -0.2865 \end{bmatrix}, C_{f2} = \begin{bmatrix} -0.0257 & -0.2738 \end{bmatrix}$$

$$D_{f1} = -0.0270, \ D_{f2} = -0.0098, \ M = 0.7211.$$

Assume the initial state of the plant and the filter are $x(0) = \tilde{x}(0) = [0.1 \ \ -0.1]^T$ and $\omega(t) = 0.2e^{-1.2t}$, the fault signal is given as

$$\theta(t) = \begin{cases} 1, & 1.5 \le t \le 2.3 \\ 0, & \text{else.} \end{cases} \quad (44)$$

In Fig. 4, the solid lines, the dash–dotted lines and the dash–dotted lines represent UMF, LMF, and weighted membership functions, respectively. Fig. 5 shows the FDF input $y(t_k)$ and the output of the plant $y(t)$, from which one can see $y(t)$ at instant t_k is sampled when the WHI from $t - \varrho$ to t satisfies the event triggering condition. Also, it can be observed that the duration of each packet at releasing instant is different due to the implementation of the adaptive METM. Fig. 6 depicts releasing instants and releasing intervals, from which one can draw a same conclusion as well. The disturbance and the fault are mainly occurred within 0–3 s. From Fig. 6, one can see that the number of releasing packets within 0–3 s is 17, accounting for 54.8% of data packets within 10 s. It illustrates that the filter receives more packets from the plant via

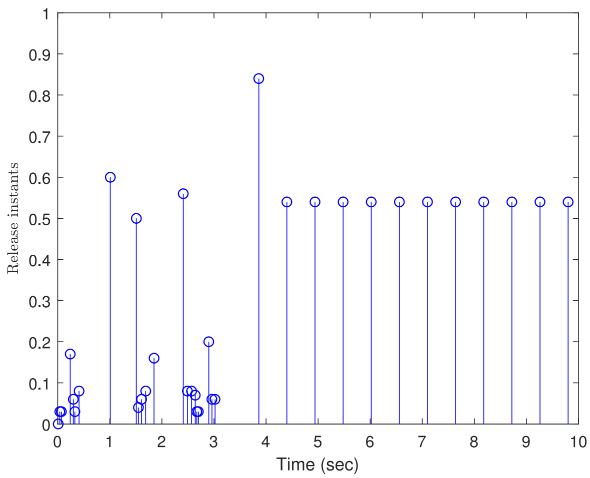

Fig. 6. Releasing sequence under the proposed adaptive METM.

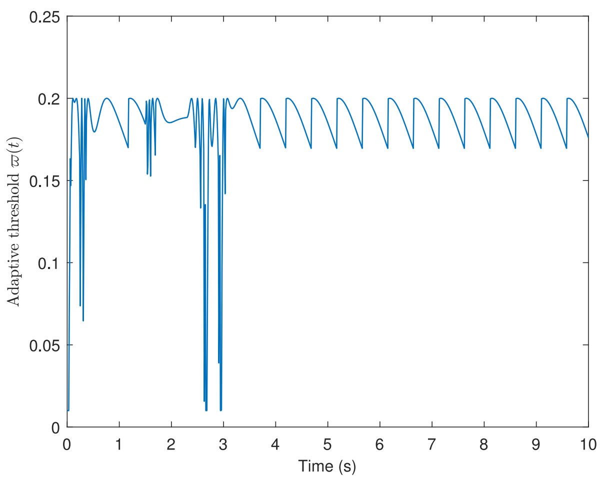

Fig. 7. Adaptive threshold of the METM.

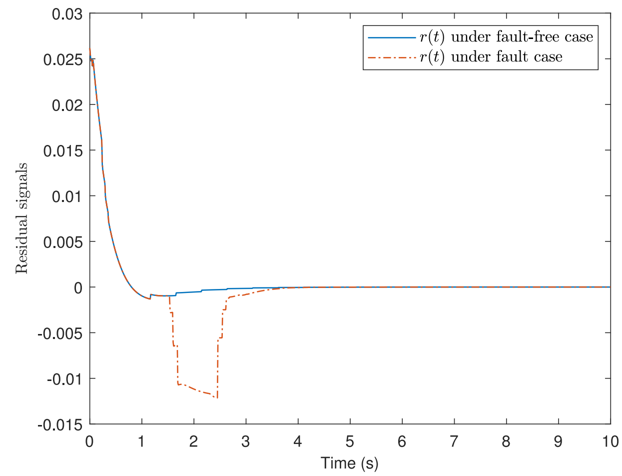

Fig. 8. Residual signal $r(t)$.

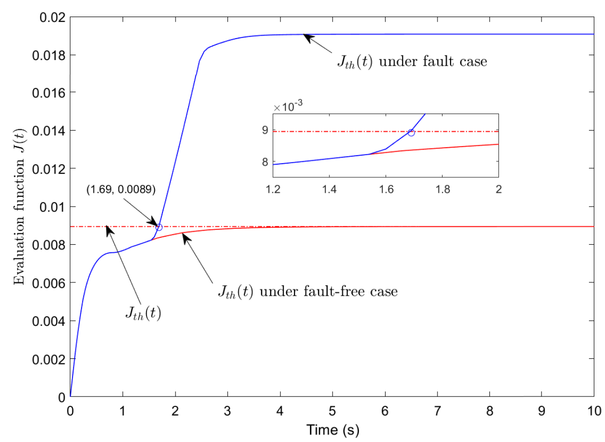

Fig. 9. Evaluation function $J(t)$.

network to achieve a better evaluation result during the system with disturbances and faults. In Fig. 7, the adaptive threshold is presented. It is clear that the greater the variation of the plant output becomes, the lower the threshold is. When the system tends to be stable after 4 s, the threshold varies from 0.16 to 0.2. Therefore, the data releasing rate can be adjusted adaptively according to the necessity of the FDF performance and the releasing requirement.

Figs. 8 and 9 show the responses of the residual signal and the evaluation function under the fault and fault-free cases, respectively. According to (9), we can calculate the FD threshold $J_{\mathrm{th}} = 0.0089$. The fault in (44) applied to the system is occurred at 1.5 s. From the response of $J(t)$, one can see that $J(t)|_{t>1.69} > J_{\mathrm{th}}$, that is to say, the fault is detected after 0.19 s according to the FD logic in (19). It demonstrates that the proposed method can lead to a satisfactory FD performance.

To illustrate the effect of parameter ϱ on the number of triggering events, Table III lists experimental results with different values of ϱ, from which one can see that a large scale of sliding window ϱ may reduce the sensitivity of event-triggering.

Next, we consider the following two ETMs: 1) the normal ETM with the format (45) and 2) the adaptive ETM formulated by (46)

TABLE III
NUMBER OF TRIGGERING EVENTS UNDER DIFFERENT ϱ

ϱ	0.03	0.06	0.15
The number of triggering events	43	38	31

TABLE IV
NUMBER OF TRIGGERING EVENTS UNDER DIFFERENT ETMs

Methods	Triggering times
Normal ETM	54
Adaptive ETM	43
Our Adaptive METM	31

$$\text{Normal ETM:} \quad t_{k+1} = \inf_{t>t_k}\left\{t|\hat{\phi}(\varepsilon(t), y(t_k)) > 0\right\} \tag{45}$$

with $\hat{\phi}(\hat{\varepsilon}(t), y(t_k)) = \hat{\varepsilon}^T(t)M\hat{\varepsilon}(t) - \varpi y^T(t_k)My(t_k)$, where $\hat{\varepsilon}(t) = y(t) - y(t_k)$ and ϖ is a constant

$$\text{Adaptive ETM:} \quad t_{k+1} = \inf_{t>t_k}\left\{t|\tilde{\phi}(\varepsilon(t), y(t_k)) > 0\right\} \tag{46}$$

with $\tilde{\phi}(\tilde{\varepsilon}(t), y(t_k)) = \tilde{\varepsilon}^T(t)M\tilde{\varepsilon}(t) - \varpi(t)y^T(t_k)My(t_k)$, where $\tilde{\varepsilon}(t) = y(t) - y(t_k)$ and $\varpi(t)$ takes the same as (10).

The comparison among the numbers of triggering events using different mechanisms are listed in Table IV, from which one can see that our proposed adaptive METM generates fewer triggering events compared with the others.

V. Conclusion

The networked FD problem has been investigated for IT2 fuzzy systems in this study. The WHI is utilized in the design of the adaptive METM to replace the current measured output of the plant. It can further reduce the data releasing rate and enhance the robustness of the METM, while maintaining the FD performance. Moreover, the adaptive threshold that depends on the WHI is designed to adjust the generation of triggering events dynamically. Considering the uncertainty of the premise variables and unmatched membership function, UMF/LMF and slack matrix technology have been utilized to improve FD evaluation performance. In addition, a hardware-in-loop simulation platform has been built to implement the signal transmission, which is mainly composed of the Arduino and ZigBee modules. Simulation results have shown the effectiveness of the proposed scheme. In future work, the METM-based fault-tolerance control will be considered and the optimal design of ϱ in the proposed METM will be studied.

References

[1] H. Chen and B. Jiang, "A review of fault detection and diagnosis for the traction system in high-speed trains," *IEEE Trans. Intell. Transp. Syst.*, vol. 21, no. 2, pp. 450–465, Feb. 2020.

[2] Y.-L. Wang and Q.-L. Han, "Network-based fault detection filter and controller coordinated design for unmanned surface vehicles in network environments," *IEEE Trans. Ind. Informat.*, vol. 12, no. 5, pp. 1753–1765, Oct. 2016.

[3] D. S. Pillai and N. Rajasekar, "A comprehensive review on protection challenges and fault diagnosis in PV systems," *Renewable Sustain. Energy Rev.*, vol. 91, pp. 18–40, Aug. 2018.

[4] R. Isermann, "Model-based fault-detection and diagnosis–Status and applications," *Annu. Rev. Control*, vol. 29, no. 1, pp. 71–85, 2005.

[5] S. Dong, Z.-G. Wu, P. Shi, H. R. Karimi, and H. Su, "Networked fault detection for Markov jump nonlinear systems," *IEEE Trans. Fuzzy Syst.*, vol. 26, no. 6, pp. 3368–3378, Dec. 2018.

[6] W.-J. Lin, Y. He, C.-K. Zhang, L. Wang, and M. Wu, "Event-triggered fault detection filter design for discrete-time memristive neural networks with time delays," *IEEE Trans. Cybern.*, early access, Aug. 12, 2020, doi: 10.1109/TCYB.2020.3011527.

[7] Y. Han, W. Qi, N. Ding, and Z. Geng, "Short-time wavelet entropy integrating improved LSTM for fault diagnosis of modular multilevel converter," *IEEE Trans. Cybern.*, early access, Jan. 5, 2021, doi: 10.1109/TCYB.2020.3041850.

[8] Y. Shen, Z.-G. Wu, P. Shi, and G. Wen, "Dissipativity based fault detection for 2D Markov jump systems with asynchronous modes," *Automatica*, vol. 106, pp. 8–17, Aug. 2019.

[9] Z. Wang, P. Shi, and C.-C. Lim, "$H\_/H_\infty$ fault detection observer in finite frequency domain for linear parameter-varying descriptor systems," *Automatica*, vol. 86, pp. 38–45, Dec. 2017.

[10] X. He, Z. Wang, Y. Ji, and D.-H. Zhou, "Robust fault detection for networked systems with distributed sensors," *IEEE Trans. Aerosp. Electron. Syst.*, vol. 47, no. 1, pp. 166–177, Jan. 2011.

[11] Z. Mao, B. Jiang, and P. Shi, "Protocol and fault detection design for nonlinear networked control systems," *IEEE Trans. Circuits Syst. II, Exp. Briefs*, vol. 56, no. 3, pp. 255–259, Mar. 2009.

[12] F. Boem, R. M. Ferrari, C. Keliris, T. Parisini, and M. M. Polycarpou, "A distributed networked approach for fault detection of large-scale systems," *IEEE Trans. Autom. Control*, vol. 62, no. 1, pp. 18–33, Jan. 2017.

[13] W. Zhang, M. S. Branicky, and S. M. Phillips, "Stability of networked control systems," *IEEE Control Syst. Mag.*, vol. 21, no. 1, pp. 84–99, Feb. 2001.

[14] P. Antsaklis and J. Baillieul, "Special issue on technology of networked control systems," *Proc. IEEE*, vol. 95, no. 1, pp. 5–8, Jan. 2007.

[15] X.-M. Zhang *et al.*, "Networked control systems: A survey of trends and techniques," *IEEE/CAA J. Autom. Sin.*, vol. 7, no. 1, pp. 1–17, Jan. 2020.

[16] R. Yang, G.-P. Liu, P. Shi, C. Thomas, and M. V. Basin, "Predictive output feedback control for networked control systems," *IEEE Trans. Ind. Electron.*, vol. 61, no. 1, pp. 512–520, Jan. 2014.

[17] X. Wang and M. D. Lemmon, "Event-triggering in distributed networked control systems," *IEEE Trans. Autom. Control*, vol. 56, no. 3, pp. 586–601, Mar. 2011.

[18] D. Yue, E. Tian, and Q.-L. Han, "A delay system method for designing event-triggered controllers of networked control systems," *IEEE Trans. Autom. Control*, vol. 58, no. 2, pp. 475–481, Feb. 2013.

[19] Y.-X. Li, Z. Hou, W.-W. Che, and Z.-G. Wu, "Event-based design of finite-time adaptive control of uncertain nonlinear systems," *IEEE Trans. Neural Netw. Learn. Syst.*, early access, Feb. 12, 2021, doi: 10.1109/TNNLS.2021.3054579.

[20] M. Gao, L. Sheng, D. Zhou, and Y. Niu, "Event-based fault detection for T–S fuzzy systems with packet dropouts and (x, v)-dependent noises," *Signal Process.*, vol. 138, pp. 211–219, Sep. 2017.

[21] Y.-L. Wang, P. Shi, C.-C. Lim, and Y. Liu, "Event-triggered fault detection filter design for a continuous-time networked control system," *IEEE Trans. Cybern.*, vol. 46, no. 12, pp. 3414–3426, Dec. 2016.

[22] S. Yan, M. Shen, S. K. Nguang, and G. Zhang. "Event-triggered H_∞ control of networked control systems with distributed transmission delay," *IEEE Trans. Autom. Control*, vol. 65, no. 10, pp. 4295–4301, Oct. 2020.

[23] Z. Gu, P. Shi, D. Yue, and Z. Ding, "Decentralized adaptive event-triggered H_∞ filtering for a class of networked nonlinear interconnected systems," *IEEE Trans. Cybern.*, vol. 49, no. 5, pp. 1570–1579, May 2019.

[24] Y. Xu, J. Sun, G. Wang, and Z.-G. Wu, "Dynamic triggering mechanisms for distributed adaptive synchronization control and its application to circuit systems," *IEEE Trans. Circuits Syst. I, Reg. Papers*, vol. 68, no. 5, pp. 2246–2256, May 2021.

[25] X.-G. Guo, X. Fan, and C. K. Ahn, "Adaptive event-triggered fault detection for interval type-2 T–S fuzzy systems with sensor saturation," *IEEE Trans. Fuzzy Syst.*, vol. 29, no. 8, pp. 2310–2321, Aug. 2021, doi: 10.1109/TFUZZ.2020.2997515.

[26] L. Zhang, H. Liang, Y. Sun, and C. K. Ahn, "Adaptive event-triggered fault detection scheme for semi-Markovian jump systems with output quantization," *IEEE Trans. Syst., Man, Cybern., Syst.*, vol. 51, no. 4, pp. 2370–2381, Apr. 2021, doi: 10.1109/TSMC.2019.2912846.

[27] J. Cheng, W. Huang, H.-K. Lam, J. Cao, and Y. Zhang, "Fuzzy-model-based control for singularly perturbed systems with nonhomogeneous Markov switching: A dropout compensation strategy," *IEEE Trans. Fuzzy Syst.*, vol. 30, no. 2, pp. 530–541, Feb. 2022, doi: 10.1109/TFUZZ.2020.3041588.

[28] Y. Xu *et al.*, "Event-triggered output synchronization for nonhomogeneous agent systems with periodic denial-of-service attacks," *Int. J. Robust Nonlinear Control*, vol. 31, no. 6, pp. 1851–1865, Apr. 2021, doi: 10.1002/rnc.5223.

[29] X.-J. Li and G.-H. Yang, "Fault detection in finite frequency domain for Takagi-Sugeno fuzzy systems with sensor faults," *IEEE Trans. Cybern.*, vol. 44, no. 8, pp. 1446–1458, Aug. 2014.

[30] H. Li, Y. Gao, L. Wu, and H.-K. Lam, "Fault detection for T–S fuzzy time-delay systems: delta operator and input-output methods," *IEEE Trans. Cybern.*, vol. 45, no. 2, pp. 229–241, Feb. 2015.

[31] S. Sun, H. Zhang, C. Liu, and Y. Liu, "Dissipativity-based intermittent fault detection and tolerant control for multiple delayed uncertain switched fuzzy stochastic systems with unmeasurable premise variables," *IEEE Trans. Cybern.*, early access, Jan. 8, 2021, doi: 10.1109/TCYB.2020.3041125.

[32] Q. Liang and J. M. Mendel, "Interval type-2 fuzzy logic systems: Theory and design," *IEEE Trans. Fuzzy Syst.*, vol. 8, no. 5, pp. 535–550, Oct. 2000.

[33] R. Sakthivel, R. Kavikumar, A. Mohammadzadeh, O.-M. Kwon, and B. Kaviarasan, "Fault estimation for mode-dependent IT2 fuzzy systems with quantized output signals," *IEEE Trans. Fuzzy Syst.*, vol. 29, no. 2, pp. 298–309, Feb. 2021.

[34] H. Li, C. Wu, L. Wu, H.-K. Lam, and Y. Gao, "Filtering of interval type-2 fuzzy systems with intermittent measurements," *IEEE Trans. Cybern.*, vol. 46, no. 3, pp. 668–678, Mar. 2016.

[35] C. Wu, H. Li, H.-K. Lam, and H. R. Karimi, "Fault detection for nonlinear networked systems based on quantization and dropout compensation: An interval type-2 fuzzy-model method," *Neurocomputing*, vol. 191, pp. 409–420, May 2016.

[36] M. Wang, G. Feng, H. Yan, J. Qiu, and H. Zhang, "Membership-function-dependent fault detection filtering design for interval type-2 ts fuzzy systems in finite frequency domain," *IEEE Trans. Fuzzy Syst.*, vol. 29, no. 9, pp. 2760–2773, Sep. 2021, doi: 10.1109/TFUZZ.2020.3006987.

[37] R. Kavikumar, R. Sakthivel, O.-M. Kwon, and B. Kaviarasan, "Robust model reference tracking control for interval type-2 fuzzy stochastic systems," *IET Control Theory Appl.*, vol. 14, no. 9, pp. 1123–1134, Jun. 2020.

[38] Y. Pan and G.-H. Yang, "Event-triggered fault detection filter design for nonlinear networked systems," *IEEE Trans. Syst., Man, Cybern., Syst.*, vol. 48, no. 11, pp. 1851–1862, Nov. 2018.

[39] H. D. Tuan, P. Apkarian, T. Narikiyo, and Y. Yamamoto, "Parameterized linear matrix inequality techniques in fuzzy control system design," *IEEE Trans. Fuzzy Syst.*, vol. 9, no. 2, pp. 324–332, Apr. 2001.

[40] H.-K. Lam and L. D. Seneviratne, "Stability analysis of interval type-2 fuzzy-model-based control systems," *IEEE Trans. Syst., Man, Cybern. B, Cybern.*, vol. 38, no. 3, pp. 617–628, Jun. 2008.

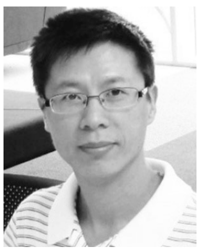

Zhou Gu (Member, IEEE) received the B.S. degree in automation from North China Electric Power University, Beijing, China, in 1997, and the M.S. and Ph.D. degrees in control science and engineering from the Nanjing University of Aeronautics and Astronautics, Nanjing, China, in 2007 and 2010, respectively.

From September 1999 to January 2013, he was with the School of Power engineering, Nanjing Normal University, Nanjing, as an Associate Professor. He is currently a Professor with Nanjing Forestry University, Nanjing. His current research interests include networked control systems, time-delay systems, reliable control, and their applications.

Dong Yue (Fellow, IEEE) received the Ph.D. degree in control theory and engineering from the South China University of Technology, Guangzhou, China, in 1995.

He is currently a Professor and the Dean of the Institute of Advanced Technology, Nanjing University of Posts and Telecommunications, Nanjing, China, and a Changjiang Professor with the Department of Control Science and Engineering, Huazhong University of Science and Technology, Wuhan, China. He has published more than 200 papers in international journals, domestic journals, and international conferences. His research interests include analysis and synthesis of networked control systems, multiagent systems, optimal control of power systems, and Internet of Things.

Prof. Yue is an Associate Editor of the IEEE TRANSACTIONS ON INDUSTRIAL INFORMATICS and the *International Journal of Systems Science*.

Ju H. Park (Senior Member, IEEE) received the Ph.D. degree in electronics and electrical engineering from the Pohang University of Science and Technology (POSTECH), Pohang, Republic of Korea, in 1997.

From May 1997 to February 2000, he was a Research Associate with the Engineering Research Center–Automation Research Center, POSTECH. He joined Yeungnam University, Gyeongsan, Republic of Korea, in March 2000, where he is currently the Chuma Chair Professor. He has coauthored the monographs *Recent Advances in Control and Filtering of Dynamic Systems With Constrained Signals* (New York, NY, USA: Springer-Nature, 2018) and *Dynamic Systems With Time Delays: Stability and Control* (New York, NY, USA: Springer-Nature, 2019). His research interests include robust control and filtering, neural/complex networks, fuzzy systems, multiagent systems, and chaotic systems. He has published a number of articles in these areas.

Prof. Park has been a recipient of the Highly Cited Researchers Award by Clarivate Analytics (formerly, Thomson Reuters) since 2015 and is listed in three fields, engineering, computer sciences, and mathematics, in 2019, 2020, and 2021. He is an Editor of an edited volume *Recent Advances in Control Problems of Dynamical Systems and Networks* (New York, NY, USA: Springer-Nature, 2020). He also serves as an Editor for the *International Journal of Control, Automation and Systems*. He is also a Subject Editor/Advisory Editor/Associate Editor/Editorial Board Member of several international journals, including *IET Control Theory & Applications, Applied Mathematics and Computation*, *The Journal of the Franklin Institute*, *Nonlinear Dynamics*, *Engineering Reports*, *Cogent Engineering*, the IEEE TRANSACTIONS ON FUZZY SYSTEMS, IEEE TRANSACTIONS ON NEURAL NETWORKS AND LEARNING SYSTEMS, and IEEE TRANSACTIONS ON CYBERNETICS. He is also a Fellow of the Korean Academy of Science and Technology.

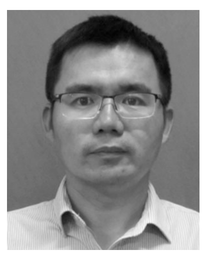

Xiangpeng Xie (Member, IEEE) received the B.S. and Ph.D. degrees in engineering from Northeastern University, Shenyang, China, in 2004 and 2010, respectively.

From 2010 to 2014, he was a Senior Engineer with Metallurgical Corporation of China Ltd., Beijing, China. He is currently a Professor with the Institute of Advanced Technology, Nanjing University of Posts and Telecommunications, Nanjing, China. His research interests include fuzzy modeling and control synthesis, state estimation, optimization in process industries, and intelligent optimization algorithms.

Prof. Xie serves as an Associate Editor for the *International Journal of Fuzzy Systems* and the *International Journal of Control, Automation, and Systems*.